Supramolecular Chemistry, 2013
Vol. 25, No. 5, 269–275, http://dx.doi.org/10.1080/10610278.2013.766735

Taylor & Francis
Taylor & Francis Group

RESEARCH ARTICLE

A clickable, highly soluble oligopeptide that easily forms organogels

Ruiying Gong[a], Yubao Song[b], Zongxia Guo[a], Ming Li[b], Yi Jiang[a] and Xiaobo Wan[a]*

[a]*Qingdao Institute of Bioenergy and Bioprocess Technology, Chinese Academy of Sciences, 189 Songling Road, Qingdao, Shandong Province 266101, P.R. China;*
[b]*Department of Chemistry, Qingdao University of Science and Technology, 53 Zhengzhou Road, Qingdao, Shandong Province 266042, P.R. China*

(*Received 19 November 2012; final version received 11 January 2013*)

An artificial peptide, N_3-GVGV-OMe (G, glycine; V, valine), which mimics the repeating GAGA (A, alanine) sequence in Bombix Mori silk, was synthesised via solution-phase synthesis. Compared with N_3-GAGA-OMe sequence, N_3-GVGV-OMe showed high solubility in common organic solvents (such as $CHCl_3$, THF and CH_2Cl_2), and easily formed organogels simply by adding poor solvents (such as toluene or ether) to the peptide solution at room temperature. The hierarchical nanostructure of N_3-GVGV-OMe organogel was dependent on the nature of the poor solvents, although in all cases, β-sheets were formed exclusively. Gels formed in ether showed higher level hierarchical assembly, as evidenced by AFM and CD studies. Solution-state FT-IR analysis showed that the pre-organisation of the peptides in solution was not significant, and well-defined antiparallel β-sheets were formed after the addition of the poor solvent. The high solubility and strong tendency for self-assembly of N_3-GVGV-OMe, together with its terminal azide group, might facilitate the modification of functional organic molecules even macromolecules for better nanostructure control.

Keywords: organogel; nanostructure; self-assembly

Introduction

Biomacromolecules, such as DNA and proteins, are perfect models in nature that achieve elegant functions by self-assembly. A long-term goal in material science is to learn from nature how to precisely control the properties of synthesised small organic molecules or macromolecules by self-assembly. Low-molecular weight oligopeptides, inspired from the repeating units in proteins, are still of interest as organogelators (*1–3*). For instance, GAGA sequence, presented in silk protein as the repeating unit, forms antiparallel β-sheet structures by self-assembly (*4–6*). It was used to adjust the nanostructure of conventional synthetic polymers (*7–9*) and π-conjugated oligomers (*10–14*). These reports strongly supported the use of oligopeptides as versatile building blocks for facilitating self-assembled supramolecular structures with definite properties. However, the tendency of self-assembly of β-sheet forming oligopeptides is also a double-edged sword: in many cases, it dramatically decreases the solubility of those oligopeptides in common organic solvents. For example, a modified GAGA tetrapeptide which mimicked Bombix Mori silk showed poor solubility in most of organic solvents (*15*, *16*). Long alphatic chains (*17*) were needed to increase its solubility. This problem presents obstacles in utilising such oligopeptides to modify small molecules or macromolecules in large scale.

We herein report the synthesis and self-assembly behaviour of an artificial tetrapeptide sequence (N_3-GVGV-OMe), which could be considered as a surrogate of the GAGA sequence. It showed excellent solubility in common organic solvents such as $CHCl_3$, CH_2Cl_2 and tetrahydrofuran (THF), and easily formed organogels at room temperature (rt) just by adding poor solvents to the peptide solution. Atomic Force Microscopy (AFM) and Circular Dichroism (CD) studies showed that the hierarchical nanostructure of the gels was dependent on the nature of the poor solvent. The N-terminal of this peptide was modified with an azide moiety, which we believe will facilitate the modification of functionalised organic molecules even macromolecules via 'click chemistry'.

Experimental

Tetrapeptide synthesis

Three tetrapeptides, namely N_3-GVGV-OMe, N_3-GAGA-OMe and butyryl-GVGV-OMe (as shown in Scheme 1), were synthesised by solution-phase peptide synthesis methodology. All the reactants used for peptide synthesis were purchased from commercial suppliers and used as received. Solvents such as CH_2Cl_2 and THF was pre-dried before use. All glasswares were thoroughly oven-dried.

*Corresponding author. Email: wanxb@qibebt.ac.cn

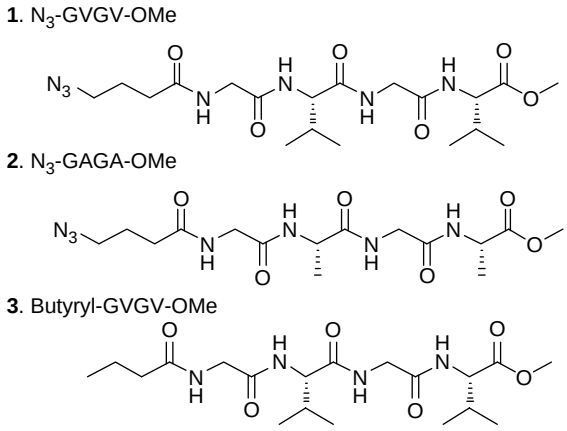

Scheme 1. Molecular structures of tetrapeptides synthesised.

The detail synthetic route towards tetrapeptide N_3-GVGV-OMe is shown in Scheme 2. N_3-GAGA-OMe and butyryl-GVGV-OMe were synthesised in a similar manner and their characterisation was provided in the Supplementary Information.

*Boc-GV-OMe (compound **6**)*

Boc-glycine (compound **4**, 3.50 g, 0.02 mol) was dissolved in 40 mL of dry CH_2Cl_2 at 0°C. HOBt (1-hydroxybenzotrizole) (2.97 g, 1.1 equiv.) and EDC·HCl (1-ethyl-3-(3-dimethyllaminopropyl) carbodiimide hydrochloride) (4.22 g, 1.1 equiv.) were added to the above solution and stirred for 15 min, followed by the addition of the valine methyl ester **5** (2.62 g, 1.0 equiv.). The solution was stirred at rt overnight. The mixture was washed with brine, and the organic layer was separated and concentrated under vacuum. The crude product was eluted by flash chromatography (ethyl acetate/petroleum ether) to afford compound **6** (5.42 g) in 94% yield.

*Boc-GV-COOH (compound **7**)*

To a 25 mL of methanol solution of Boc-GV-OMe (compound **6**, 2.88 g, 0.01 mol) was added lithium hydroxide (3.78 g, 9.0 equiv.) all at once. The solution was stirred at rt overnight. The pH value of reaction mixture was adjusted to 1 with diluted HCl solution and the resulting mixture was extracted with CH_2Cl_2 three times. The combined CH_2Cl_2 layers were dried over anhydrous $MgSO_4$ and concentrated under reduced pressure to afford compound **7** (2.60 g) in 95% yield.

NH_2-GV-OMe *(compound **8**)*

Boc-GV-OMe (compound **6**, 0.14 g, 0.5 mmol) was dissolved in 10 mL of CH_2Cl_2 and then 1 mL of trifluoroacetic acid (TFA) was added. The solution was stirred at rt overnight. The solvent was removed to afford a syrup in almost quantitative yield. The crude product was used in the next step without further purification.

*Boc-GVGV-OMe (compound **9**)*

Boc-GV-COOH (compound **7**, 5.49 g, 0.02 mol) was dissolved in 40 mL of dry CH_2Cl_2 at 0°C. HOBt

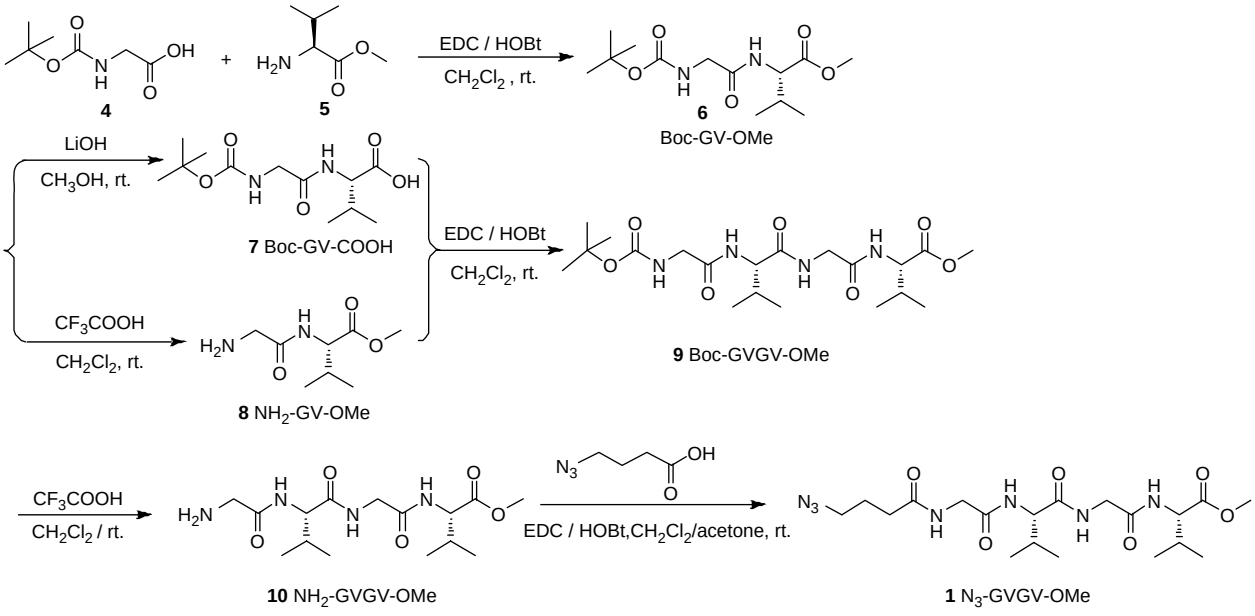

Scheme 2. The synthetic routes of stepwise synthesis of tetrapeptide N_3-GVGV-OMe.

(1.1 equiv.) and EDC·HCl (1.1 equiv.) were added to the above solution and stirred for 15 min, followed by the addition of NH_2-GV-OMe (compound **8**, 3.76 g, 1.0 equiv.). The solution was stirred at rt overnight. The organic layer was then washed with brine and concentrated under reduced pressure. The crude product was purified by flash chromatography (ethyl acetate/petroleum ether) to give compound **9** (7.64 g) in 86% yield.

NH_2-GVGV-OMe *(compound **10**)*

Boc-GVGV-OMe (compound **9**, 0.22 g, 0.5 mmol) was dissolved in 10 mL of CH_2Cl_2 and then 1 mL of TFA was added. The solution was stirred at rt overnight. The solvent was removed to afford a syrup in almost quantitative yield. The residue was used for further synthesis without further purification.

N_3-GVGV-OMe *(compound **1**)*

4-Azidobutyric acid (1.29 g, 0.01 mol) was dissolved in 35 mL of dry CH_2Cl_2 at 0°C. HOBt (1.49 g, 1.1 equiv.) and EDC·HCl (2.11 g, 1.1 equiv.) were added to the above solution and stirred for 15 min, followed by the addition of NH_2-GVGV-OMe (compound **10**, 3.44 g, 1.0 equiv.). The solution was stirred at rt overnight. The reaction mixture was pipetted into 200 mL of Et_2O and the resulting white gel was filtered and dried under reduced pressure to afford compound **1** (3.19 g) in 70% yield.

Gel formation

Typical method to prepare N_3-GVGV-OMe gel in toluene: 3.3 mg of N_3-GVGV-OMe was dissolved in 0.1 mL of $CHCl_3$ to afford a transparent solution. To this solution, 0.9 mL toluene was added dropwise. The gel formation was confirmed by vial inversion method.

Typical example of formation of N_3-GVGV-OMe gel in Et_2O: 6.9 mg of N_3-GVGV-OMe was dissolved in 0.4 mL of $CHCl_3$ to afford a transparent solution. To this solution, 0.4 mL of Et_2O was added dropwise. The gel formation was confirmed by vial inversion method.

Characterisation

FT-IR analysis was carried out on Nicolet 6700 FT-IR Spectrometer. Freshly prepared N_3-GVGV-OMe solution (in $CHCl_3$) was used for solution-state FT-IR analysis. Xerogel samples for FT-IR were prepared simply by drying the wet gels under reduced pressure for 15 h. AFM was carried out on Agilent 5400 using tapping mode. SEM was carried out on Hitachi S-4800 with an accelerating voltage of 2.5 kV. The fresh prepared organogel was casted on freshly cleaved mica, dried under reduced pressure for 15 h, and then used for characterisations of AFM and SEM. CD spectra were measured with JASCO-815 spectrophotometer. The prepared gel was casted onto a quartz slide and dried in a vacuum oven for 15 h. UV–vis spectra of N_3-GVGV-OMe in $CHCl_3$ and N_3-$(CH_2)_4$-COOH were recorded on Cary 50 UV-Vis spectrophotometer. HRMS (EI) were carried out on Bruker maXis Q-TOF mass spectrometer.

Results and discussions

The goal of this research was to find a short peptide sequence that fulfilled three criteria: (a) it was easily self-assembled into β-sheets, (b) it was highly soluble in organic solvents and (c) it had an anchor that can be attached to other molecules in high yield. For efficient self-assembly in organic solvents, a tetrapeptide was estimated to be sufficient (*17*). Although the GAGA sequence was widely used with different materials to regulate their assembly behaviours (*8*, *15*, *16*, *18–20*), compared with L-valine, L-alanine was a weaker β-sheets former (*21*). It was reasonable to postulate that tetrapeptide GVGV, with the alanine residue replaced with a valine residue, would not deteriorate the β-sheets formation ability. Moreover, since valine residues bear larger hydrophobic side chains (isopropyl) than alanine (methyl), the replacement might increase the solubility of the peptide in organic solvents.

Actually, a pentapeptide, GVGVP (P, proline), was found as a part of the repeating sequences in elastin (*22*). However, it did not show good self-assembly properties due to the presence of proline at the end of the sequence (*23*). We envisioned that the removal of proline from this sequence would reinstall its ability to form β-sheets. 4-Azidobutyric acid was chosen as the anchor to introduce the azide group to the N-terminal of the peptide.

Thus, N_3-GVGV-OMe (compound **1**) was synthesised via conventional solution-phase peptide synthesis, as shown in Scheme 2. N_3-GAGA-OMe (compound **2**), which mimicked the key repeating unit in Bombix Mori silk, and butyryl-GVGV-OMe (compound **3**), which was used to investigate the role of the azide group in self-assembly, were also synthesised in a similar manner (details available in Supplementary Information) for comparison.

Solubility and gel formation ability

Since good solubility of the oligopeptides in organic solvents is one of the key factors to make them applicable in modification of functionalised materials, we explored in detail the solubility of all three peptides (results, see Table S1 of the Supplementary Information, available online). We were surprised to find that N_3-GVGV-OMe and butyryl-GVGV-OMe showed excellent solubility in

common organic solvents such as CH_2Cl_2, $CHCl_3$, THF and dimethylformamide (DMF) at rt. In sharp contrast, N_3-GAGA-OMe was only soluble in polar organic solvents such as DMF and dimethyl sulfoxide (DMSO). It is not surprising that GAGA type tetrapeptides showed poor solubility as evidenced in the literature (*15*, *16*).The improvement of the peptide solubility in organic solvents by switching alanine residue to valine residue might be attributed to the larger hydrophobic isopropyl group in valine. The solubility of N_3-GVGV-OMe was even up to 650 mg/mL in $CHCl_3$, which is an obvious advantage to use this peptide to modify other functional molecules for inducing the self-assembly thereof. We noticed that some oligopeptides for self-assembly studies were also reported to be soluble in common organic solvents, but all with bulky Boc protecting group on N-terminals to increase its solubility (*24*, *25*).

Moreover, unlike most of peptides, which had to be dissolved in hot solvents and then cooled down to rt to form organogel, N_3-GVGV-OMe formed organogel simply by adding poor solvents (ether or toluene) to the peptide solution (in $CHCl_3$, CH_2Cl_2 DMF or THF) at rt. On the other hand, the solution of N_3-GAGA-OMe failed to form organogels when poor solvents were added, and only a precipitate was observed instead (see Table S2 of the Supplementary Information, available online). This result indicated that when the alanine moiety in the GAGA sequence was replaced by valine, the tetrapeptide showed better ability to gelate organic solvents. To the best of our knowledge, the oligopeptide gel formation by adding a poor solvent to a peptide solution at rt was scarcely reported, which might be due to the poor solubility of the peptides. A phenylalanine dipeptide formed organogels when it was firstly dissolved in 1,1,1,3,3,3-hexafluoropropanol and then diluted with poor solvent (*26*). Fmoc-protected dipeptides formed hydrogels when first dissolved in DMSO and then diluted with water (*27*). In both cases, a highly polar solvent had to be used to dissolve the peptide. In our case, a wide variety of organic solvents could be used to dissolve N_3-GVGV-OMe and all formed organogels easily by adding poor solvents. The minimum gelation concentration (MGC) of N_3-GVGV-OMe was in mg/mL scale (e.g. MGC in $CHCl_3$/toluene was 3.3 mg/mL).

Interestingly, although butyryl-GVGV-OMe also showed good solubility in $CHCl_3$, no obvious gelation formation was observed by adding ether or toluene to its $CHCl_3$ solution. This suggested that the azide group also contributed to the self-assembly of tetrapeptide, maybe via $\pi-\pi$ stacking from azide groups (*28*, *29*). The formation of organogel for N_3-GVGV-OMe but not for N_3-GAGA-OMe or butyryl-GVGV-OMe indicated that a delicate balance between H-bonding, hydrophobic–hydrophobic interactions and $\pi-\pi$ stacking was needed to achieve better self-assembly.

We also noticed that the polymorphism of the gel was strongly influenced by the poor solvents. Regardless the type of good solvents used to dissolve the peptide, gels formed in ether were opaque while gels formed in toluene were transparent, which inferred the existence of different hierarchical nanostructures. An example (images of organogels obtained in $CHCl_3/Et_2O$ and $CHCl_3$/toluene, insertion) is shown in Figure 1. The difference in gel polymorphism was studied by AFM. Figure 1(a) clearly showed that the organogel formed in $CHCl_3/Et_2O$ consisted of both thin and thick fibrils. An enlarged image (Figure 1(b)) showed that a thick left-handed-helices fibre (*ca*. 45 nm in width and 25 nm in pitch) was a higher level hierarchical structure, composed of at least two or more twisted filaments. The AFM images of organogel obtained in $CHCl_3$/toluene (Figure 1(c)), on the other hand, showed more uniformed but thinner nanofibres. SEM images (see Figure S1 of the Supplementary Information, available online) also gave similar results. The difference in the nanostructures of the same oligopeptide in different solvents showed that the self-assembly process was strongly dependent on solvents (*30*, *31*). The coexistence of both thin and thick nanofibres in organogel formed in $CHCl_3/Et_2O$ might be accounted for its opaque appearance, which was supported by a recent

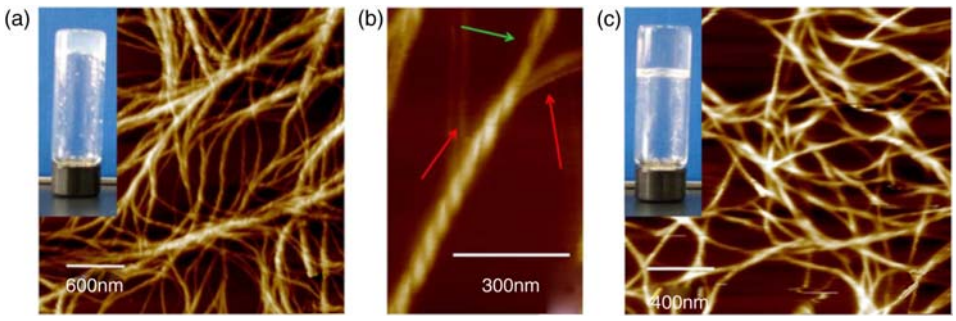

Figure 1. AFM images of N_3-GVGV-OMe xerogels obtained in $CHCl_3/Et_2O$ (gel concentration: 8.6 mg/mL) (a and b) and in $CHCl_3$/toluene (gel concentration: 3.3 mg/mL). (c) The images of the organogels were inserted at the up left corner in (a) and (c).

report on the polymorph changes of gels formed at different temperatures (*32*).

FT-IR study on the gel formation

Despite their appearance differences, the nanofibres obtained in both gel systems consisted mostly of β-sheets, as indicated by FT-IR analysis. It was generally accepted that the absorptions in the amide A, amide I and amide II regions were indicative for peptide's secondary structures, such as α-helix and β-sheet (*33*). The non-assembled peptides normally had absorptions at 3412–3426 cm^{-1} (amide A), 1659–1678 cm^{-1} (amide I) and 1503–1516 cm^{-1} (amide II), while peptides forming β-sheet showed absorptions at ~3280, ~1630 and ~1540 cm^{-1}. Figure 2 showed the IR spectra of the xerogels of N_3-GVGV-OMe obtained in different gelation systems. All the xerogels showed very similar absorption peaks, regardless of the solvents. The absorptions at 3281, 1627 and 1544 cm^{-1} clearly indicated the formation of β-sheet, and the weak absorption at 1688 cm^{-1} inferred that the β-sheet was in an antiparallel manner (*33*). No characteristic peaks of either α-helix or random coil were seen in these spectra, indicating the strong tendency towards antiparallel β-sheet formation of this oligopeptide.

It would be interesting to investigate how the antiparallel β-sheet was formed: whether there was a pre-organisation of the oligopeptide in the solution and the nanofibre was formed simply because of the solubility decrease due to the addition of the poor solvent, or the peptide was reorganised and formed β-sheet after the addition of poor solvent? So, the solution-state FT-IR spectra of N_3-GVGV-OMe at different concentrations ranging from 1.1 to 33.0 mg/mL in $CHCl_3$ solution were recorded and analyzed

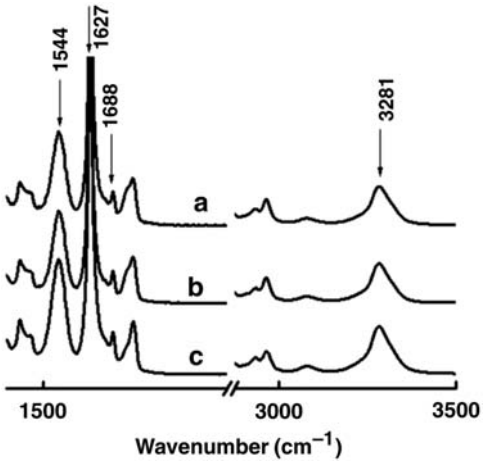

Figure 2. FT-IR spectra of N_3-GVGV-OMe xerogels obtained in: (a) THF/toluene (gel concentration: 3.3 mg/mL), (b) $CHCl_3$/toluene (gel concentration: 3.3 mg/mL) and (c) $CHCl_3/Et_2O$ (gel concentration: 8.6 mg/mL).

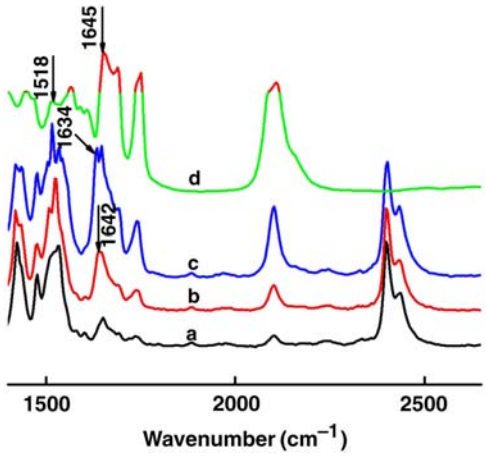

Figure 3. FT-IR spectra of N_3-GVGV-OMe in $CHCl_3$ solution at different concentrations: (a) 1.1 mg/mL, (b) 3.3 mg/mL, (c) 9.0 mg/mL and (d) 33.0 mg/mL.

(as shown in Figure 3). Since $CHCl_3$ showed a broad absorption around 3000 cm^{-1} (see Figure S2 of the Supplementary Information, available online), which overlapped with the absorption of N_3-GVGV-OMe in this region, only the absorption evolution in amide I and amide II regions was discussed. At lower concentrations, the broad absorption around 1642 cm^{-1} was predominant in amide I region, which was not a typical antiparallel β-sheet absorption, indicating that the pre-organisation of the peptide into antiparallel β-sheet was not obvious (Figure 3(a),(b)). At higher concentrations, certain degree of assembly appeared, as evidenced by the splitting of the absorptions in amide I region, but the non-bonded peptide absorptions, for example absorption at 1518 cm^{-1}, still existed (Figure 3(c)). When the concentration was increased to 33.0 mg/mL, the formation of β-sheet still could not be clearly observed (Figure 3(d)). Hence, the addition of the poor solvent was the major reason for the formation of well-organised β-sheet structure in gels. This observation was different from the reported pre-organisation of oligopeptides to form β-sheet in solution before the gel was formed (*33–35*).

Circular dichroism study on the details of the self-assembly

Xerogels were placed perpendicular to the light path and rotated with a constant speed within the film plane to avoid polarisation-dependent reflections and eliminate the possible angle dependence of CD signal (*36*). Normally, peptides which formed β-sheets had a weak positive CD signal around 190–195 nm and a stronger negative peak around 220 nm. However, for the gels obtained from $CHCl_3$/toluene, the characteristic peak around 220 nm for β-sheets was barely seen (Figure 4(a)), maybe due to the overlap with the strong azide absorption at 228 nm

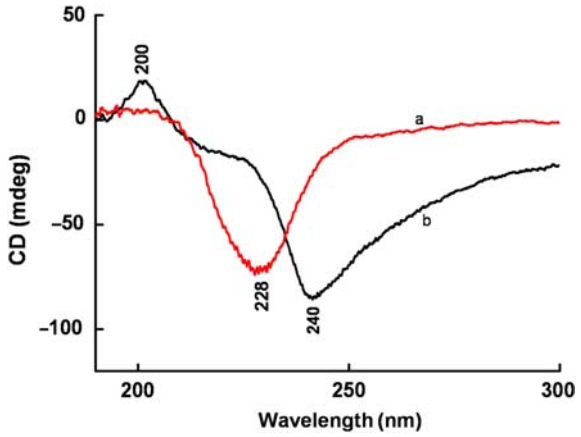

Figure 4. CD spectra of of N_3-GVGV-OMe xerogel obtained in (a) $CHCl_3$/toluene (gel concentration: 3.3 mg/mL) and (b) $CHCl_3/Et_2O$ (gel concentration: 8.6 mg/mL).

(azide group has a strong absorption around 230 nm, see Figure S3 of the Supplementary Information, available online). The strong negative azide absorption peak indicated that the azide groups were stacked in a chiral environment. However, a positive peak at 200 nm and a negative shoulder around 220 nm were seen in the CD spectrum for xerogel obtained from $CHCl_3/Et_2O$ system (Figure 4(b)), which was indicative for the existence of β-sheets. Interestingly, the azide absorption was shifted from 228 to 240 nm, indicating the existence of subtle nanostructure differences caused by switching poor solvent from toluene to ether. Although FI-IR suggested β-sheets were formed in all the cases, the redshift of the azide peak indicated better stacked azide groups in the organogel obtained from $CHCl_3/Et_2O$ system. This is in accordance with its higher level hierarchical nanostructure observed in AFM study.

Possible explanation for gel formation

As described in previous sections, slight structural changes dramatically changed the ability of the peptide to form organogels. H-bonding, $\pi-\pi$ stacking and hydrophobic–hydrophobic interaction have to be dedicately balanced to achieve good self-assembly. N_3-GAGA-OMe was unable to form organogels, which was ascribed to weaker hydrophobic–hydrophobic interactions compared with N_3-GVGV-OMe; butyryl-GVGV-OMe also failed to form hydrogels, which might be due to the absence of azide–azide interaction. Azid–azide interactions were observed in both organic molecules and organic–inorganic complexes, hence also played an important role here in the tetrapeptide assembly (*28*, *29*, *37*). A plausible stacking model is proposed in Scheme 3 to explain the gel formation process. These nanofibrils of N_3-GVGV-OMe in organogels state were composed of stacks of molecules formed from coefficient interaction of H-bonding and $\pi-\pi$ stacking direction. The different gelation states of N_3-GVGV-OMe in Et_2O and toluene might also be explained by $\pi-\pi$ stacking: stronger azide stacking in ether would be expected since Et_2O would not interfer with azide group; on the other hand, toluene, which is able to interact with azide group via $\pi-\pi$ stacking (*37*), would weaken the $\pi-\pi$ stacking between azide groups. As shown in Scheme 3, $\pi-\pi$ stacking might play an important role for β-sheets to form large bundles. This might explain why larger bundles were formed when Et_2O was used as poor solvent but not in the case of toluene. Given that if the nanostructure was not altered during xerogel preparation, this also would explain the bathochromic shift of the azide absorption in CD spectra.

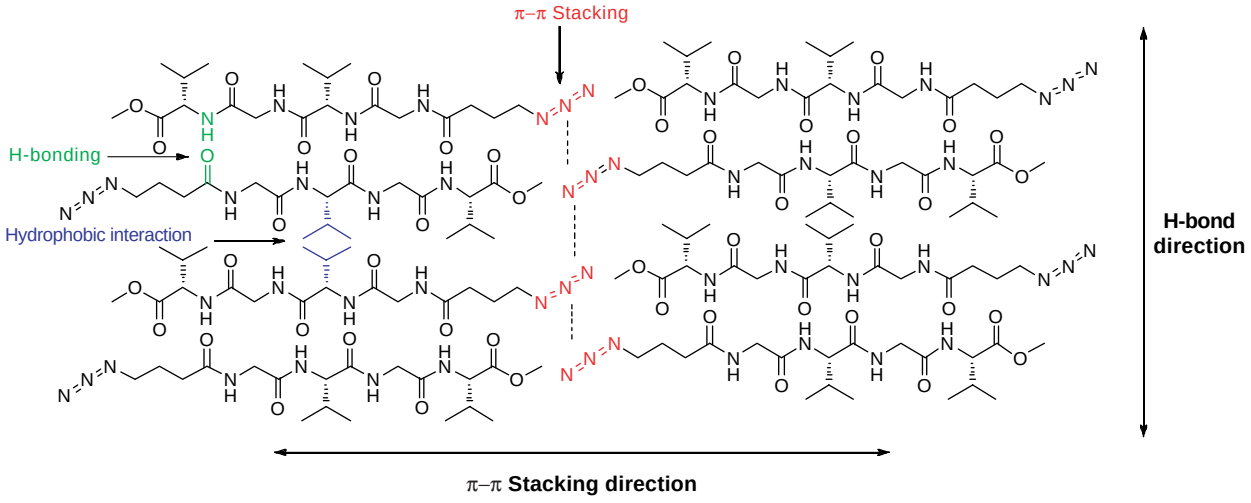

Scheme 3. Plausible stacking model for antiparallel β-sheet formation.

Conclusion

In summary, N_3-GVGV-OMe, an artificial tetrapeptide which mimics GAGA sequence in Bombix Mori silk, was rationally designed and synthesised. It showed good solubility in most of organic solvents, and easily formed organogels when poor solvent was added to the peptide solution at rt. However, N_3-GAGA-OMe sequence was only soluble in highly polar organic solvent such as DMSO and DMF, and failed to form organogel when added to poor solvent. This indicated that the artificial tetrapeptide showed better gelation ability than the natural one under the same preparation conditions. This might be attributed to the replacement of alanine moiety with valine moiety, which not only increased the solubility of the peptide sequence, but also offered stronger hydrophobic–hydrophobic interactions which favoured the formation of organogels. Further investigation showed that the terminal azide group also contributed to the gel formation. Solution-state FT-IR suggested that the formation of well-defined β-sheets was induced by the addition of poor solvents. Analysis showed that although all the nanofibres in the gel consisted of antiparallel β-sheets, the fine nanostructure was dependent on the nature of the poor solvents. Nanofibres obtained in ether showed higher level hierarchical assembly, as evidenced by AFM and CD studies. We are currently exploring the applications of this tetrapeptide in modifying conjugated polymers and other functional materials for better nanostructure control.

Acknowledgements

This work is fanancially supported by '100 Talents Program' from the Chinese Accademy of Sciences, and Natural Science Foundation of Shandong Province (ZR2010BZ007, BS2009CL026 and Y2008B03). We are also very grateful for helpful discussions and advice from Prof. Minghua Liu at the Institute of Chemistry, Chinese Academy of Sciences.

References

(1) Maity, S.; Kumar, P.; Haldar, D. *Soft Matter.* **2011**, *7*, 5239–5245.
(2) Adhikari, B.; Nanda, J.; Banerjee, A. *Chem. Eur. J.* **2011**, *17*, 11488–11496.
(3) Lagadec, C.; Smith, D.K. *Chem. Commun.* **2011**, *47*, 340–342.
(4) Becker, N.; Oroudjev, E.; Mutz, S.; Cleveland, J.P.; Hansma, P.K.; Hayashi, C.Y.; Makarov, D.E.; Hansma, H.G. *Nat. Mater.* **2003**, *2*, 278–283.
(5) Shao, Z.; Vollrath, F. *Nature* **2002**, *418*, 741.
(6) Vollrath, F.; Knight, D.P. *Nature* **2001**, *410*, 541–548.
(7) Winningham, M.J.; Sogah, D.Y. *Macromolecules* **1997**, *30*, 862–876.
(8) Rathore, O.; Sogah, D.Y. *Macromolecules* **2001**, *34*, 1477–1486.
(9) Rathore, O.; Sogah, D.Y. *J. Am. Chem. Soc.* **2001**, *123*, 5231–5239.
(10) Klok, H.A.; Rosler, A.; Gotz, G.; Mena-Osteritz, E.; Bauerle, P. *Org. Biomol. Chem.* **2004**, *2*, 3541–3544.
(11) Matmour, R.; De Cat, I.; George, S.J.; Adriaens, W.; Leclere, P.; Bomans, P.H.H.; Sommerdijk, N.A.J.M.; Gielen, J.C.; Christianen, P.C.M.; Heldens, J.T.; van Hest, J.C.M.; Lowik, D.W.P.M.; De Feyter, S.; Meijer, E.W.; Schenning, A.P.H.J. *J. Am. Chem. Soc.* **2008**, *130*, 14576–14583.
(12) Diegelmann, S.R.; Gorham, J.M.; Tovar, J.D.J. *Am. Chem. Soc.* **2008**, *130*, 13840–13841.
(13) Stone, D.A.; Hsu, L.; Stupp, S.I. *Soft Matter.* **2009**, *5*, 1990–1993.
(14) Schillinger, E.K.; Mena-Osteritz, E.; Hentschel, J.; Börner, H.G.; Bäuerle, P. *Adv. Mater.* **2009**, *21*, 1562–1567.
(15) Escuder, B.; Miravet, J.F. *Langmuir* **2006**, *22*, 793–797.
(16) Iqbal, S.; Miravet, J.F.; Escuder, B.; Eur. *J. Org. Chem.* **2008**, *27*, 4580–4590.
(17) Jahnke, E.; Millerioux, A.S.; Severin, N.; Rabe, J.P.; Frauenrath, H. *Macromol. Biosci.* **2007**, *7*, 136–143.
(18) Liu, H.T.; Xu, W.L.; Zhao, S.P.; Huang, J.J.; Yang, H.J.; Wang, Y.L.; Ouyang, C.X. *J. Appl. Polym. Sci.* **2010**, *117*, 235–242.
(19) Vandermeulen, G.W.M.; Kim, K.T.; Wang, Z.; Manners, I. *Biomacromolecules* **2006**, *7*, 1005–1010.
(20) Hwang, W.; Kim, B.H.; Dandu, R.; Cappello, J.; Ghandehari, H.; Seog, J. *Langmuir* **2009**, *25*, 12682–12686.
(21) Pashuck, E.T.; Cui, H.G.; Stupp, S.I. *J. Am. Chem. Soc.* **2010**, *132*, 6041–6046.
(22) Foster, J.A.; Bruenger, E.; Gray, W.R.; Sandberg, L.B. *J. Biol. Chem.* **1973**, *248*, 2829–2876.
(23) Ma, M.; Kuang, Y.; Gao, Y.; Zhang, Y.; Gao, P.; Xu, B. *J. Am. Chem. Soc.* **2010**, *132*, 2719–2728.
(24) Das, A.K.; Banerjee, A. *Macromol. Symp.* **2006**, *241*, 14–22.
(25) Banerjee, A.; Palui, G. *Soft Matter.* **2008**, *4*, 1430–1437.
(26) Yan, X.; Cui, Y.; He, Q.; Wang, K.; Li, J. *Chem. Mater.* **2008**, *20*, 1522–1526.
(27) Chen, L.; Raeburn, J.; Sutton, S.; Spiller, D.G.; Williams, J.; Sharp, J.S.; Griffiths, P.C.; Heenan, R.K.; King, S.M.; Paul, A.; Furzeland, S.; Atkins, D.; Adams, D.J. *Soft Matter* **2011**, *7*, 9721–9727.
(28) Tosin, M.; Müller-Bunz, H.; Murphy, P.V. *Chem. Commun.* **2004**, 494–495.
(29) Xia, Q.; Xiao, H.; Ju, X.; Tan, J.; Gong, X.; Ji, G. *J. Chin. Chem. Soc* **2003**, *50*, 757–764.
(30) Jonkheijm, P.; Vander Schoot, P.; Schenning, A.P.; Meijer, E.W. *Science* **2006**, *313*, 80–83.
(31) Castelletto, V.; Hamley, I.W.; Harris, P.J.F.; Olsson, U.; Spencer, N. *J. Phys. Chem. B.* **2009**, *113*, 9978–9987.
(32) Nebot, V.J.; Armengol, J.; Smets, J.; Prieto, S.F.; Escuder, B.; Miravet, J.F. *Chem. Eur. J.* **2012**, *18*, 4063–4072.
(33) Yamada, N.; Ariga, K.; Naito, M.; Matsubara, K.; Koyama, E. *J. Am. Chem. Soc.* **1998**, *120*, 12192–12199.
(34) Tzokova, N.; Fernyhough, C.M.; Topham, P.D.; Sandon, N.; Adams, D.J.; Butler, M.F.; Armes, S.P.; Ryan, A.J. *Langmuir* **2009**, *25*, 2479–2485.
(35) Kotharangannagari, V.K.; Sánchez-Ferrer, A.; Ruokolainen, J.; Mezzenga, R. *Macromolecules* **2012**, *45*, 1982–1990.
(36) Spitz, C.; Dähne, S.; Ouart, A.; Abraham, H.W. *J. Phys. Chem. B.* **2000**, *104*, 8664–8669.
(37) Tosin, M.; Murphy, P.V. *J. Org. Chem.* **2005**, *70*, 4107–4117.